Interactions between Small Amphipathic Molecules and Proteins

By M. N. Jones and A. Brass

DEPARTMENT OF BIOCHEMISTRY AND MOLECULAR BIOLOGY, UNIVERSITY OF MANCHESTER, MANCHESTER M13 9PT

1 Introduction

Food emulsions and foams are generally stabilized by the adsorption of surface-active materials at the aqueous–oil and aqueous–air interfaces, respectively. These materials are often proteins or low molecular weight amphipathic emulsifiers (surfactants) or a combination of both these species.[1,2] Proteins and emulsifiers not only compete for adsorption sites at the interfaces but interact in the bulk aqueous phase to form a range of protein–surfactant complexes which are themselves surface active. Thus, it is important for understanding the stabilization of food emulsions and foams that the interactions between the proteins and surfactants which lead to the formation of such complexes are characterized.

Protein–surfactant interactions have been extensively studied by a variety of experimental methods.[3–5] It is established that surfactants can be broadly divided into those which complex to proteins and initiate unfolding of the tertiary structure (denaturing surfactants) and those in which the tertiary structure is maintained (non-denaturing surfactants). The commonly used anionic surfactants, *e.g.* sodium n-dodecylsulphate (SDS) or n-dodecylsulphonate, fall into the former category; the nonionic surfactants, *e.g.* the Tritons or n-octyl-β-glucoside (OBG), fall into the latter category, and, when used to solubilize cellular systems, they disperse membrane lipids and membrane proteins without substantial loss of enzymic activity.[6,7] It should, however, be noted that there are significant exceptions to the above generalization. The anionic amphipathics, sodium cholate and deoxycholate, which are related to the 'biological surfactant' bile salts[8] are non-denaturing. There are also some proteins which are resistant to denaturation by even powerful denaturants such as SDS under certain conditions, *e.g.* papain, pepsin and bacterial catalase,[9,10] and there are cases of surfactant activation of enzymes, *e.g.* *Aspergillus niger* catalase is activated by SDS,[11] glucose-6-phosphatase by Triton X-100,[12] and phospholipase by deoxycholate.[13]

Apart from the above exceptions, the general pattern of protein–surfactant interactions can be broadly depicted as in Figure 1, in which the surfactant ligand

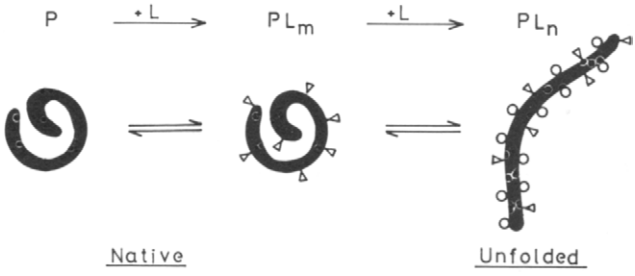

Figure 1 *A schematic representation of the binding of surfactant ligands* L *to the native state of a protein* P *and the subsequent unfolding process*

initially binds to sites on the surface of the native protein. For anionic surfactants, this initial interaction will involve the cationic amino-acid residues of lysine, histidine, and arginine, whereas for non-ionics the binding sites will be hydrophobic patches on the protein surface. In the case of non-ionics, binding ceases once such sites are occupied, but for ionic surfactants the protein unfolds exposing the hydrophobic interior and numerous potential binding sites. Saturation of all the binding sites generally occurs below the critical micelle concentration (CMC) of the surfactant, and on a weight basis this corresponds to approximately 1–2 grams of surfactant per gram of protein; the latter figure is found for reduced proteins (*i.e.* no disulphide bridges) at high ionic strength.[4] That initial binding of anionic surfactants to cationic residues occurs has been confirmed by chemical modification of the residues[14] and studies on polypeptides.[15] However, it should be noted that the ionic interaction by itself is insufficient to anchor the surfactant to the protein, and there must be an accompanying hydrophobic interaction between the alkyl chain of the surfactant and hydrophobic regions adjacent to the cationic sites on the protein surface, since the binding characteristics are dependent on the alkyl chain length.[14]

Theoretical Background—The pattern of protein–surfactant interaction is, from the theoretical viewpoint, one of multiple equilibria which can be written in terms of the protein (P), the surfactant (S), and the complexes (PS_n):

$$\begin{aligned} P + S &\rightleftharpoons PS_1 \\ PS_1 + S &\rightleftharpoons PS_2 \\ PS_2 + S &\rightleftharpoons PS_3 \\ PS_{n-1} + S &\rightleftharpoons PS_n. \end{aligned} \tag{1}$$

For such a series of equilibria, if the equilibrium constants K for each step are identical, then it follows that

$$K^n = \frac{[PS_n]}{[P][S]^n}, \tag{2}$$

and the average number of surfactant molecules bound per protein molecule $\bar{\nu}$ is given by

$$\bar{\nu} = \frac{n[PS_n]}{[P] + [PS_n]} = \frac{n(K[S])^n}{1 + (K[S])^n}. \tag{3}$$

To take into account the fact that the equilibrium constants will in general not be identical, Hill[16] suggested the equation

$$\bar{\nu} = \frac{n(K[S])^{n_H}}{1 + (K[S])^{n_H}}, \tag{4}$$

where n_H is a co-operativity coefficient and K becomes an intrinsic binding constant. For $n_H < 1$, binding is negatively co-operative (*i.e.* the binding of a ligand weakens the binding of subsequent ligands); for $n_H > 1$, binding is positively co-operative (*i.e.* the binding of a ligand enhances the binding of subsequent ligands). For identical independent binding sites we have $n_H = 1$, and then equation (4) gives rise to the Scatchard equation

$$\bar{\nu}/[S] = K(n - \bar{\nu}), \tag{5}$$

which has been extensively used by many workers despite its shortcomings as exposed and discussed by Klotz *et al.*[18–20]

Figure 2 shows model binding isotherms for a hypothetical molecule with 50 binding sites (intrinsic binding constant 10^4) for various degrees of co-operativity (n_H from 0.5 to 7.5). Apart from increasing steepness with increasing n_H, the

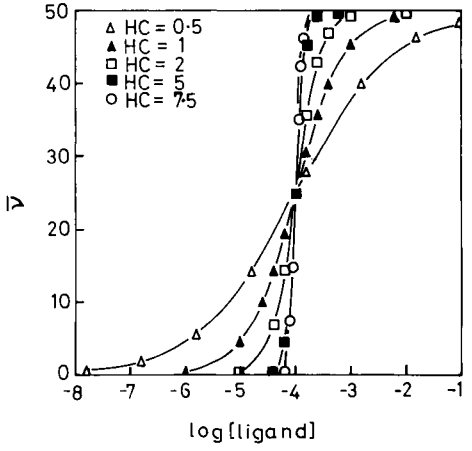

Figure 2 *Binding isotherms ($\bar{\nu}$ versus log [ligand]) calculated from the Hill equation for a protein with 50 binding sites (intrinsic binding constant 10^4) for a range of Hill coefficients from 0.5 to 7.5*

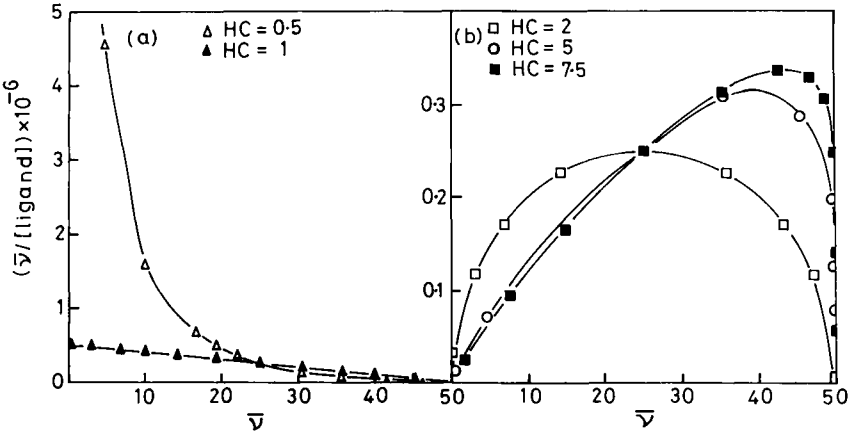

Figure 3 *Scatchard plots* $(\bar{\nu}/[ligand]_{free}$ *versus* $\bar{\nu})$ *for the isotherms of Figure 2 for a protein with 50 binding sites (intrinsic binding constant* 10^4*) for a range of Hill coefficients from 0.5 to 7.5*

curves are all qualitatively the same, *i.e.* sigmoidal. However, Scatchard plots derived from these isotherms are diagnostic of the type of co-operativity[21] (Figure 3), negative curvature and maxima being characteristic of negative and positive co-operativity, respectively. The description of multiple equilibria in terms of overall binding constants is inevitably an approximation since the binding of every surfactant ligand must change the binding constant for subsequent ligands. A procedure which enables binding constants to be determined as binding proceeds was proposed by Wyman[22] who introduced the binding potential concept.

The binding potential $\pi\ (p, T, \mu_1, \mu_2, \ldots)$ at pressure p and temperature T relates ligand binding ν to chemical potential μ as follows

$$\bar{\nu} = \left(\frac{\partial \pi}{\partial \mu}\right)_{p,T}; \tag{6}$$

and it can be calculated by integration under the binding isotherm assuming that the chemical potential of the ligand can be represented by the ideal solution expression:

$$\pi = 2.303RT \int_{\bar{\nu}=0}^{\bar{\nu}} \bar{\nu}\, \mathrm{d} \log [\mathrm{S}], \tag{7}$$

where R is the gas constant. Considering the formation of a specific complex (PS_n) by differentiating equation (3) with respect to ln [S] followed by substitution into equation (7) and integration, we have

$$\pi = RT \ln (1 + K[\mathrm{S}]^n). \tag{8}$$

At a given [S] corresponding to a given $\bar{\nu}$, if $PS_{\bar{\nu}}$ is the predominant species, it follows that

$$\pi = RT \ln (1 + K_{app}[S]^{\bar{\nu}}). \tag{9}$$

By calculating π from equation (7) and substituting into equation (9), the apparent binding constant K_{app} can be calculated for any given $\bar{\nu}$. Thus, the Gibbs energy 'per ligand bound' ($\Delta G_{\bar{\nu}}$) can be obtained from

$$\Delta G_{\bar{\nu}} = -\frac{RT}{\bar{\nu}} \ln K_{app}. \tag{10}$$

The plot of $\Delta G_{\bar{\nu}}$ *versus* $\bar{\nu}$ shows how successive numbers of bound ligands affect the Gibbs energy of binding. Applying the treatment to the model isotherms in Figure 2 gives the Gibbs energy profiles shown in Figure 4a. The curves converge to the expected value of $\Delta G_{\bar{\nu}}$ of -22 kJ mol^{-1} (corresponding to $K_{app} = 10^4$) on saturation of the binding sites ($\bar{\nu} = 50$), but do not reflect the trends expected from the co-operativity coefficients. For $n_H = 1$, $\Delta G_{\bar{\nu}}$ should be independent of $\bar{\nu}$, whereas, for $n_H > 1$, $\Delta G_{\bar{\nu}}$ should become more negative with increasing $\bar{\nu}$ (*i.e.* positive co-operativity). These anomalies are due to the neglect of the statistical contributions to $\Delta G_{\bar{\nu}}$ which are very significant for large numbers of binding sites. For i ligands binding to n binding sites, the number of arrangements $\Omega_{n,i}$ is given by

$$\Omega_{n,i} = \frac{n!}{(n-i)!\, i!}, \tag{11}$$

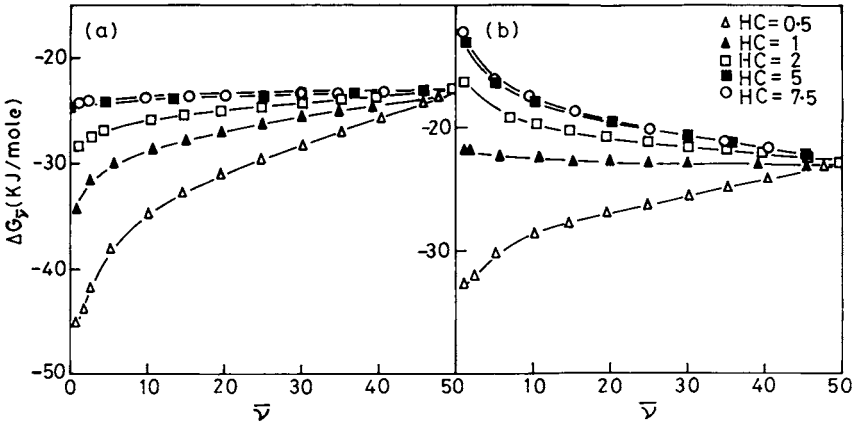

Figure 4 *Gibbs energies of binding per ligand bound* ($\Delta G_{\bar{\nu}}$ versus $\bar{\nu}$) *calculated by the Wyman binding potential method from the isotherms of Figure 2 for a protein with 50 binding sites (intrinsic binding constant* 10^4*) for a range of Hill coefficients from 0.5 to 7.5*: (a) *without statistical corrections*, (b) *with statistical corrections*

which correspond to an entropy of $R \ln \Omega_{n,i}$, and a Gibbs energy per ligand bound of $-(RT/i) \ln \Omega_{n,i}$. Applying this statistical factor to a total of 50 binding sites gives the curves shown in Figure 4b. These curves show the expected trends with variation in the Hill coefficients, *i.e.* for $n_H < 1$, $\Delta G_{\bar{\nu}}$ decreases with ν, and, for $n_H > 1$, $\Delta G_{\bar{\nu}}$ increases (becomes more negative) with $\bar{\nu}$.

2 Results and Discussion

Thermodynamics—Figure 5 shows binding isotherms for SDS and OBG binding to the globular protein lysozyme (14 306 daltons) in aqueous solutions at 25 °C. The binding isotherms for SDS at two ionic strengths (0.0119 M and 0.2119 M) are typical of the binding of an ionic surfactant to a globular protein. The initial highly co-operative (steep) part of the binding curve corresponds to specific binding of SDS to cationic sites on the protein surface. These sites saturate at $\bar{\nu} \sim 15$–20 (there are 18 cationic residues in lysozyme). Specific ionic binding is weakened on increasing the ionic strength as seen by the shift in the initial curve to higher free SDS concentration. After saturation of the cationic sites, further binding occurs as the free SDS concentration approaches the CMC. At this stage the protein has unfolded as can be shown by the development of an endothermic contribution to the enthalpy of interaction.[14] The pre-CMC rise in the binding isotherm is shifted to lower free SDS concentration on increasing the ionic strength—this is characteristic of hydrophobic interactions.

The binding of the non-ionic OBG to lysozyme shows only a hydrophobic binding region as the CMC of OBG is approached. Binding in this case has been interpreted in terms of the formation of complexes in which the OBG is bound to

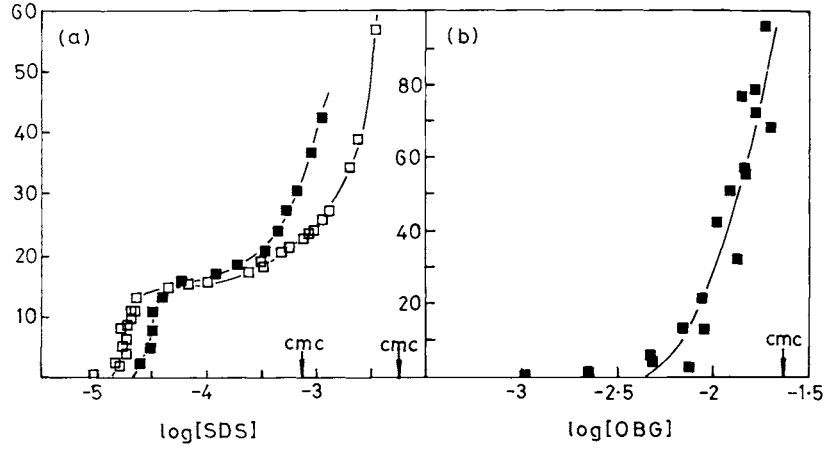

Figure 5 (a) *Binding isotherms for the binding of sodium n-dodecylsulphate to lysozyme in aqueous solution at* 25 °C, pH 3.2: □, *ionic strength* 0.0119 M; ■, *ionic strength* 0.2119 M. (b) *Binding isotherms for the binding of n-octyl-β-glucoside to lysozyme in aqueous solution at* 25 °C, pH 6.4, *ionic strength* 0.132 M

hydrophobic areas on the surface of the native protein to form a prolate ellipsoidal complex.[24] To saturate the surface of lysozyme with OBG assuming that the detergent forms a monolayer requires 114 OBG molecules.

The Hill or Scatchard equations when applied to the specific binding regions of SDS isotherms enable the calculation of intrinsic binding constants. Binding isotherms for OBG can be similarly treated. Intrinsic binding constants can be used to calculate the average Gibbs energies per surfactant bound ($\Delta G_{\bar{\nu}}$) over the range of $\bar{\nu}$ values from which they are derived. Table 1 shows some selected thermodynamic parameters for SDS and OBG binding to several globular proteins obtained by these methods. The enthalpies of binding ($\Delta H_{\bar{\nu}}$) were obtained by microcalorimetry. The data for SDS relate to specific binding regions of the isotherms. The data for OBG relate to the whole isotherm. It is clear from these figures that $\Delta H_{\bar{\nu}}$ makes a relatively small contribution to $\Delta G_{\bar{\nu}}$, and that the specific ionic interactions are of considerably larger energy than the hydrophobic non-specific interactions which occur between the proteins and OBG. It should be noted that these methods do not take into account statistical factors.

Application of the Wyman method gives a more informative profile of the way in which $\Delta G_{\bar{\nu}}$ depends on $\bar{\nu}$ as shown in Figure 6 for the interaction of SDS with lysozyme at two ionic strengths. However, the continuous curves in such figures do not take into account statistical factors which present a particularly interesting problem when the protein unfolds. If we consider binding to the cationic sites on the native protein, then the statistical contribution can be calculated from equation (11) assuming that these sites saturate. From the binding isotherm, there are *ca.* 16–17 of such sites. The statistical contributions reduce the values of $\Delta G_{\bar{\nu}}$ (*i.e.* they are less negative), but they decrease with increasing $\bar{\nu}$ and become zero when the specific sites are saturated. When the protein unfolds the number of potential binding sites increases, thus increasing the statistical contributions. Assuming unfolding is a co-operative process, the range of $\bar{\nu}$ over which unfolding occurs will be relatively narrow, and, while we cannot define it precisely, for lysozyme calorimetric measurements[14,25] indicate that unfolding occurs very

Table 1 *Selected thermodynamic parameters for the binding of sodium n-dodecylsulphate (SDS)*[5] *and n-octyl β-glycoside*[24] *to globular proteins in aqueous solutions at* 25 °C

Protein (pH, $\bar{\nu}$)	$\Delta G_{\bar{\nu}}$	$\Delta H_{\bar{\nu}}$ (kJ mol^{-1})	$T\Delta S_{\bar{\nu}}$
Ribonuclease A–SDS (pH 7.0, 19)	−27.9	−1.27	26.6
Ribonuclease A–OBG (pH 6.4, 100)	−11.2	0.311	11.5
Lysozyme–SDS (pH 3.2, 18)	−26.2	−8.66	17.5
Lysozyme–OBG (pH 6.4, 130)	−10.2	0.783	11.0
Ovalbumin–SDS (pH 7.0, 37)	−30.0	0.0	30.0
Ovalbumin–OBG (pH 6.4, 400)	−10.9	0.202	11.1
Bovine serum albumin–SDS (pH 7, 57)	−24.8	−6.95	17.9
Bovine serum albumin–OBG (pH 6, 550)	−9.7	0.668	10.4
Bovine catalase–SDS (pH 3.2, 343)	−28.4	−8.36	20.0
Bovine catalase–OBG (pH 6.4, 1900)	−10.5	0.343	10.8

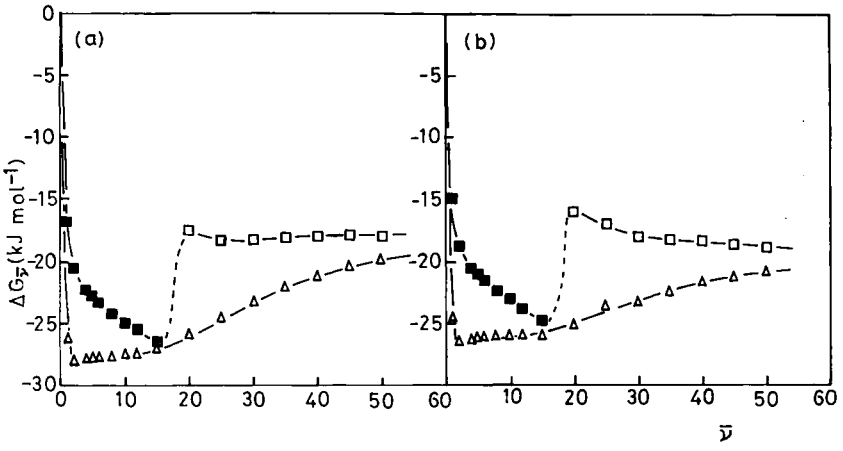

Figure 6 *Gibbs energy of binding per sodium n-dodecylsulphate ligand as a function of the number of SDS ligands bound to lysozyme in aqueous solution at* 25 °C, pH 3.2: △, *calculated from the binding potential without statistical corrections*; □,■, *calculated with statistical corrections for binding to the native* (■) *and unfolded* (□) *states*; (a) *ionic strength* 0.0119 M; (b) *ionic strength* 0.2119 M

close to the point of saturation of the specific binding sites. It seems reasonable to assume that surfactant remains bound to the specific sites after unfolding so that the statistical contributions to binding to the unfolded protein must be calculated from the difference between the number of specific binding sites and the number of binding sites at saturation. The binding isotherms suggest that the number of binding sites at saturation is *ca.* 60 (this figure corresponds to the binding of 1.2 g SDS per g of lysozyme, which is consistent with other saturation binding levels for native proteins[4]). Thus, to a first approximation, the statistical contributions to the Gibbs energies of binding to the unfolding protein should be calculated for *ca.* 45 binding sites.

Figure 6 shows that, when the statistical contributions are taken into account, the curves of $\Delta G_{\bar{\nu}}$ show a transition arising from protein unfolding. The change in $\Delta G_{\bar{\nu}}$ on unfolding can be related to the Gibbs energy of unfolding in the unliganded (ΔG_{U}) and liganded ($\Delta G_{\mathrm{U/SDS}}$) states as follows:

$$\mathrm{N} + \bar{\nu}\mathrm{SDS} \rightleftharpoons \mathrm{N(SDS)}_{\bar{\nu}} : \bar{\nu}\Delta G^{N}_{\bar{\nu}}, \tag{12}$$

$$\mathrm{U} + \bar{\nu}\mathrm{SDS} \rightleftharpoons \mathrm{U(SDS)}_{\bar{\nu}} : \bar{\nu}\Delta G^{U}_{\bar{\nu}}, \tag{13}$$

where N and U are the native and unfolded protein respectively, and $\bar{\nu}$ corresponds to the number of ligands bound at the mid-point of the transition. Thus, we have

$$\bar{\nu}(\Delta G^{\mathrm{U}}_{\bar{\nu}} - \Delta G^{\mathrm{N}}_{\bar{\nu}}) = \bar{\nu}(\delta\Delta G_{\bar{\nu}}) = \Delta G_{\mathrm{U/SDS}} - \Delta G_{\mathrm{U}}. \tag{14}$$

Table 2 *Thermodynamic parameters for the lysozyme–SDS interaction in aqueous solution* (pH 3.2) *at* 25 °C

Ionic strength (M)	$\bar{\nu}$ (*transition pt*)	$\delta\Delta G_{\bar{\nu}}$	$\bar{\nu}(\delta\Delta G_{\bar{\nu}})$	$\Delta G_U{}^*$ (kJ mol^{-1})	$\Delta G_{U/SDS}$
0.0119	17	10	170	46	216
0.0269	18	11.5	207	46	253
0.0554	17	10	170	46	216
0.1119	17	10.5	179	46	225
0.2119	18	10.5	189	46	235
Average					229 ± 16

* Ref. 26.

Table 2 shows the values of the parameters in equation (14) for the lysozyme + SDS system over a range of ionic strength. The Gibbs energy of unfolding of the liganded protein is considerably larger than that for the unliganded protein. Thus the initial binding of surfactant to the cationic sites stabilizes the native state complex, but as binding proceeds the decrease in Gibbs energy resulting from unfolding and exposure of a large number of hydrophobic binding sites more than compensates for the energy required to unfold the liganded native state. Figure 7 shows the total Gibbs energy of complex formation ($\bar{\nu}\Delta G_{\bar{\nu}}$) as a function of $\bar{\nu}$. The kink in the curves corresponds to unfolding.

Molecular Modelling—In order to gain a deeper understanding of the protein–surfactant binding process at the molecular level, computer simulations were performed of various lysozyme–SDS complexes. The dynamical behaviour of the

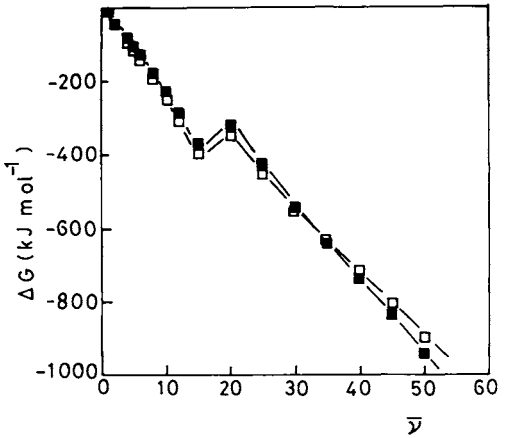

Figure 7 *Gibbs energy of formation of lysozyme–sodium-n-dodecylsulphate complexes as a function of the number of SDS ligands bound at* 25 °C, pH 3.2: □, *ionic strength* 0.0119 M, ■, *ionic strength* 0.2119 M

lysozyme–SDS complexes was modelled using the technique of molecular dynamics.[27] From a knowledge of the various potential functions describing the molecular interactions in a protein, the force on every atom in the protein at some time t can be calculated. Using Newton's equations of motion, it is therefore possible to calculate the acceleration on every atom and then to integrate iteratively the equations of motion to obtain the position of each atom at time $t + \delta t$, where δt is typically of the order 1 fs. By performing several tens of thousands of such iterations, the motion of a protein over a period of 10–1000 ps can be followed. Although this time period is very short, it is sufficient to calculate various thermodynamic properties of the lysozyme–SDS complexes.

The co-ordinates of lysozyme were taken from the Brookhaven database.[28] Because these co-ordinates are derived from *X*-ray studies, the positions of the hydrogens are not defined. Polar hydrogens were explicitly added to the structure and non-polar hydrogens were neglected. The CHARMM description of the protein potentials was used,[29] including modified potentials for carbon atoms with non-polar hydrogens. All the protein simulations were run using the POLYGEN[29] suite of programs on a Silicon Graphics 4D/240GTX graphics work station. Ideally, the lysozyme–SDS simulations would be performed in an aqueous environment by adding several thousand water molecules to the system. However, this would greatly increase the amount of time needed to perform the simulations. An aqueous environment was therefore approximated by using a radially dependent dielectric with a dielectric constant of 80 (to model the charge screening that would occur in a dielectric solvent).[30]

All simulation systems were gradually heated from 0 to 300 K in 10 ps. Each simulation was then run for a further 10 ps with the temperature maintained at 300 K in order to allow the system to equilibrate at this temperature. Each simulation was then run for a further 10 ps with no temperature rescaling to allow for further equilibration. The simulations were finally run for a further 40 ps during which time the average values of the various thermodynamic quantities were calculated.

Simulations were first made on a single molecule of lysozyme at pH 7. The structure of the lysozyme at the end of the simulation is shown in Figure 8. This structure was then protonated to match the charge state at pH 3 to correspond to the experimentally measured SDS binding data and the simulation was repeated using the final structure obtained from the pH 7 simulation as the starting configuration. Figure 9 shows the structure of lysozyme at pH 3 (averaged over the last 40 ps of the simulation). It is interesting to note that the cleft in the lysozyme closes at low pH. At no point in any of the subsequent simulations did the cleft re-open. A similar simulation was also made of an isolated SDS molecule.

A series of simulations was then made in which various numbers of SDS molecules were complexed to the lysozyme. The *X*-ray co-ordinates of lysozyme complexed with four SDS molecules are known[31] and could therefore be used to determine the initial configuration for the complexes with up to four SDS molecules. The position of other SDS binding sites could be determined by an electrostatic examination of the lysozyme molecule. It is assumed that the

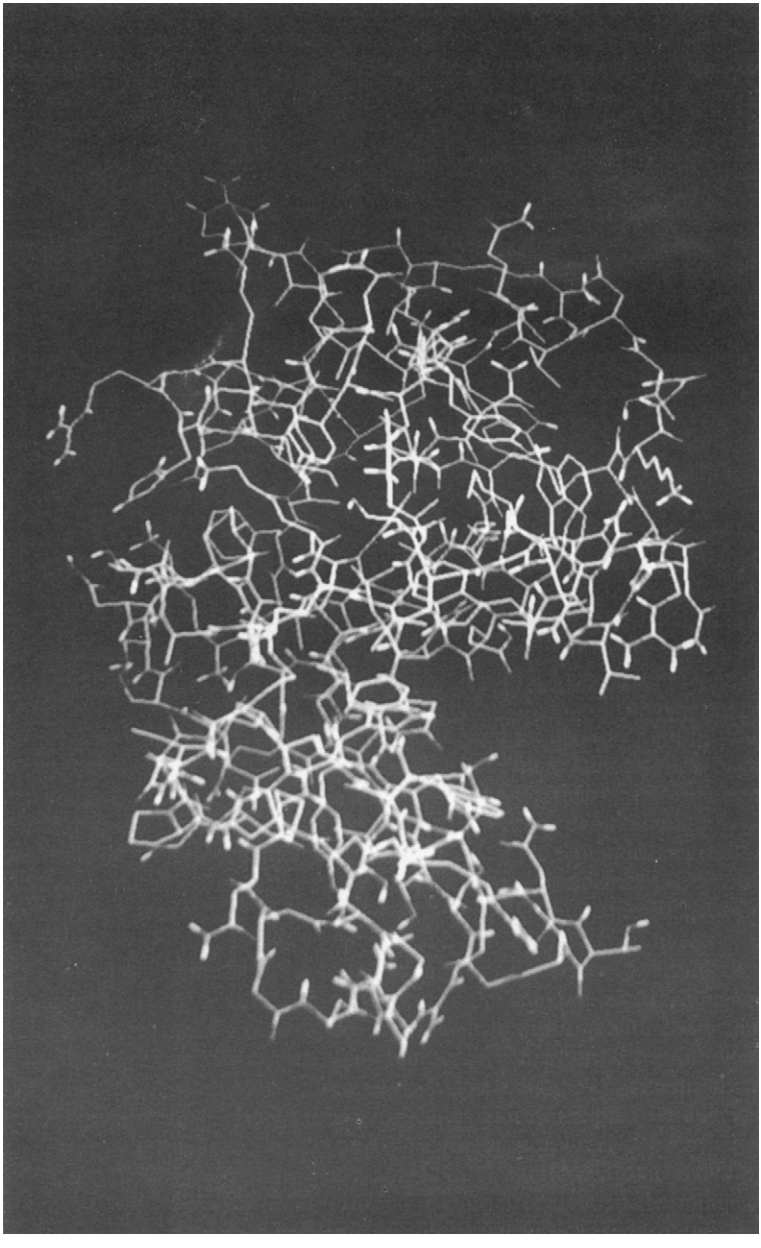

Figure 8 *The protein backbone for lysozyme at* **pH** 7 (300 K) *averaged over the last* 40 ps *of a molecular dynamics simulation*

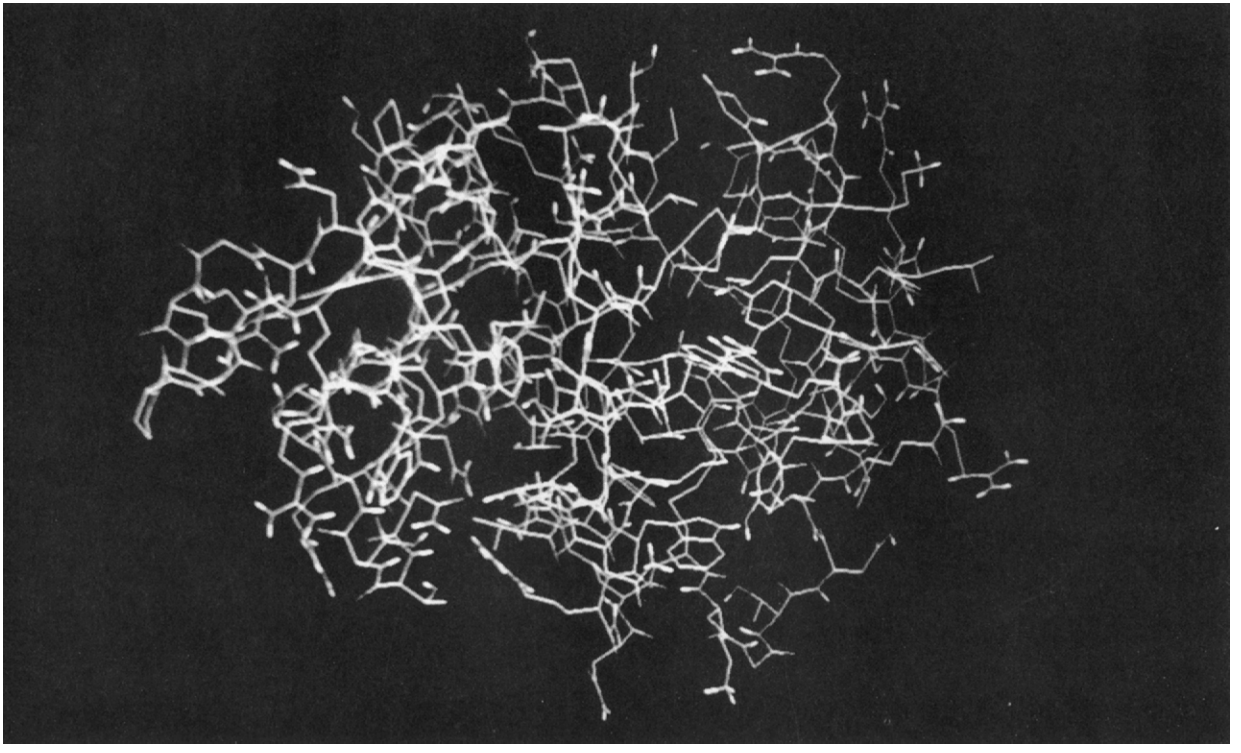

Figure 9 *The protein backbone for lysozyme at* pH 3 (300 K) *averaged over the last* 40 ps *of the simulation. The cleft seen in the structure at* pH 7 (*Figure* 8, *bottom left*) *has closed-up*

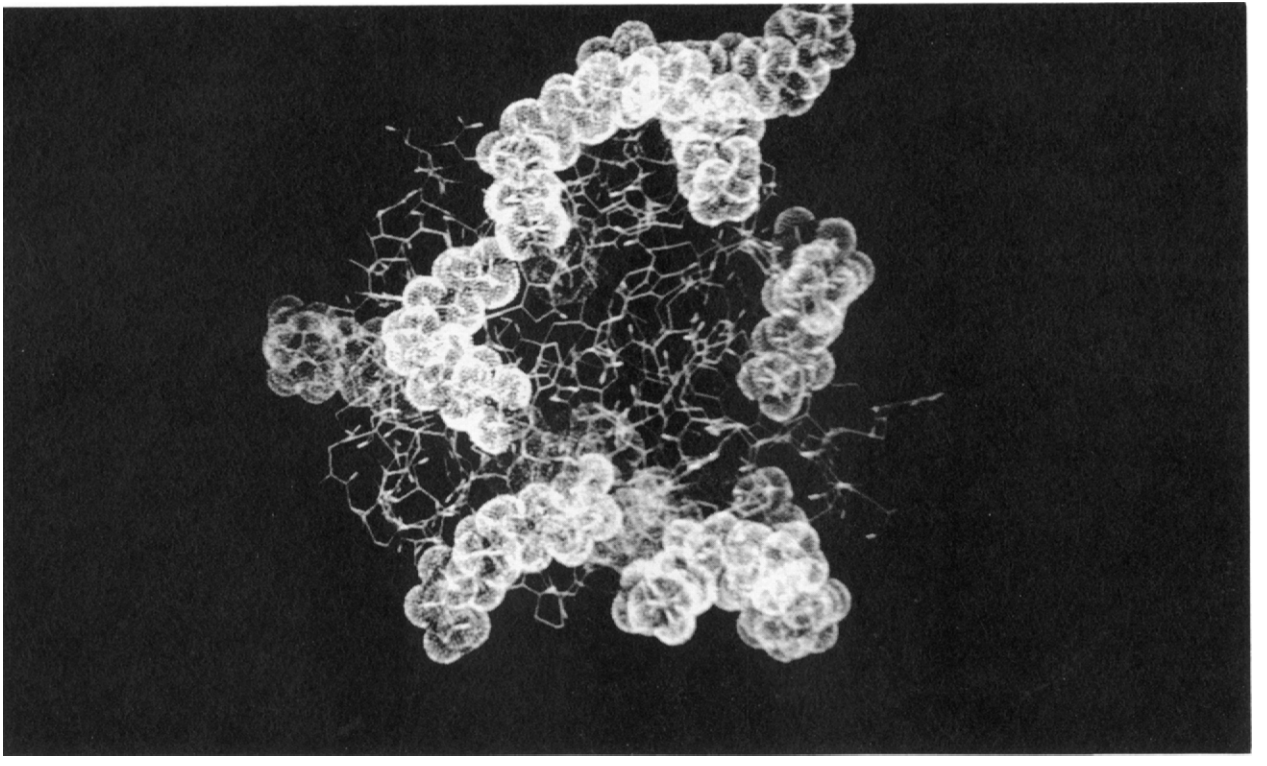

Figure 10 *The structure of lysozyme–$(SDS)_{10}$ complex at* pH 3 (300 K) *averaged over the last* 40 ps *of the simulation. The SDS molecules are depicted by van der Waals spheres*

Table 3 *The potential energy, kinetic energy, and total energy for a range of lysozyme–SDS complexes*

Complex	*Total energy* (kJ mol^{-1})	*Potential energy* (kJ mol^{-1})	*Kinetic energy* (kJ mol^{-1})
Lysozyme	6552	2029	4523
SDS	251	135	117
Lysozyme–$(SDS)_1$	6544	1948	4594
Lysozyme–$(SDS)_2$	6573	1933	4636
Lysozyme–$(SDS)_4$	7088	2151	4933
Lysozyme–$(SDS)_7$	7607	2330	5276
Lysozyme–$(SDS)_{10}$	8251	2556	5694

negatively charged head group of the SDS molecule interacts with positively charged residues, and the hydrophobic tail of SDS interacts with the hydrophobic region of the lysozyme surface. In order to determine potential SDS binding sites on the surface of lysozyme, a potential energy surface of lysozyme at pH 3 was generated using an electron as the probe charge. From this surface it was possible to predict the positions at which SDS can bind to the surface of lysozyme.

As expected, the hydrophilic head group of the SDS molecules bonded strongly to positively charged groups on the lysozyme surface, and the hydrophobic SDS tail oriented itself along hydrophobic channels on the protein surface (particularly favouring aromatic groups). The values of the potential energy, kinetic energy and total energy of the complexes with 1, 2, 4, 7, and 10 SDS molecules are shown in Table 3. Figure 10 shows a picture of the lysozyme–$(SDS)_{10}$ complex.

From the information given in Table 3, it is possible to calculate the binding energies of the SDS molecules to the lysozyme. The difference in energy between lysozyme and SDS separately and the complexes gives a measure of the binding energy of the complex [see equation (1)]. The binding energies per SDS molecule bound can then be calculated and are shown in Figure 11.

It is interesting that the shape of this simulated binding energy curve is similar to that obtained experimentally. The values of the binding energies are not, however, equivalent. This is not surprising, as the computer simulation measures the change in potential energy on binding and not the Gibbs free energy of binding which is measured experimentally. Also, the computer simulation does not explicitly include water, and so does not include the contribution to the binding energy from the making and breaking of hydrogen bonds as the surfactant molecules bind to the protein.

The distortion of the lysozyme structure by the addition of SDS molecules was measured by comparing the average protein backbone positions of the isolated lysozyme at pH 3, and the lysozyme with 10 SDS added. Figure 12 shows the protein backbone structure of lysozyme at pH 3 superimposed on the protein backbone of lysozyme with 10 SDS molecules attached. The RMS value for this displacement was found to be small, only 2.13 Å—the secondary structure of the lysozyme was maintained when 10 SDS molecules were bound to its surface. The molecular dynamics approach is now being extended to investigate the denaturation of lysozyme which is observed when larger numbers of SDS molecules are bound.

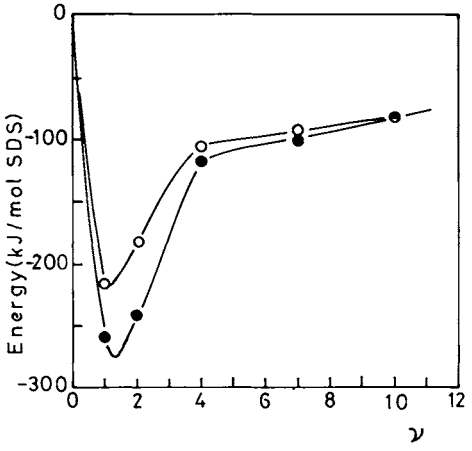

Figure 11 *Binding energy per SDS molecule calculated from the computer simulations of the energies of the lysozyme-SDS complexes as a function of the number of SDS molecules bound at* pH 3 (300 K). ●, *the binding energy measured from the differences in total energy*; ○, *the binding energies measured from the differences in potential energy*

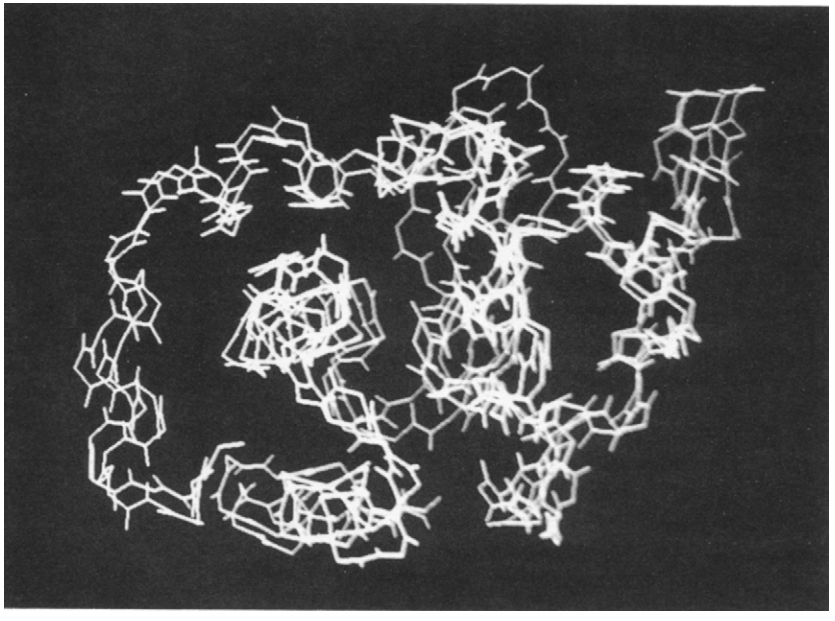

Figure 12 *The superimposed protein backbones for the average structures of lysozyme and the lysozyme–*$(SDS)_{10}$ *complex*

References

1. 'Food Emulsions and Foams', ed. E. Dickinson, Royal Society of Chemistry, London, 1987.
2. E. Dickinson and G. Stainsby, 'Colloids in Food', Applied Science, London, 1982.
3. J. Steinhardt and J. A. Reynolds, 'Multiple Equilibria in Proteins', Academic Press, New York, 1969.
4. M. N. Jones, 'Biological Interfaces', Elsevier, Amsterdam, 1975, p. 101.
5. M. N. Jones, in 'Biological Thermodynamics', ed. M. N. Jones, Elsevier, Amsterdam, 1988, p. 182.
6. A. Helenius and K. Simons, *Biochim. Biophs. Acta*, 1975, **415**, 29.
7. D. Lichtenberg, R. J. Robson, and E. A. Dennis, *Biochim. Biophys. Acta*, 1983, **737**, 285.
8. A. F. Hofmann and K. J. Mysels, *Colloids Surf.*, 1988, **30**, 145.
9. C. A. Nelson, *J. Biol. Chem.*, 1971, **246**, 3895.
10. M. N. Jones, P. Manley, P. J. W. Midgley, and A. E. Wilkinson, *Biopolymers*, 1982, **21**, 1435.
11. M. N. Jones, A. Finn, A. Mosavi-Movahedi, and B. J. Walker, *Biochim. Biophys. Acta*, 1987, **913**, 395.
12. F. E. Beyhl, *IRCS Med. Sci.*, 1986, **14**, 417.
13. M. Y. El-Sayert and M. F. Roberts, *Biochim. Biophys. Acta*, 1985, **831**, 133.
14. M. N. Jones and P. Manley, *J. Chem. Soc., Faraday Trans 2*, 1980, **76**, 654.
15. M. I. Paz-Andrade, M. N. Jones, and H. A. Skinner, *J. Chem. Soc., Faraday Trans. 1*, 1978, **74**, 2923.
16. A. V. Hill, *J. Physiol.*, 1910, **40**, 40P.
17. G. Scatchard, *Ann. N.Y. Acad. Sci.*, 1949, **51**, 660.
18. I. M. Klotz, *Science*, 1982, **217**, 1247.
19. I. M. Klotz and D. L. Hunston, *J. Biol. Chem.*, 1984, **259**, 10060.
20. H. A. Feldman, *J. Biol. Chem.*, 1983, **258**, 12865.
21. G. Schwarz, *Biophys. Struct. Mech.*, 1976, **2**, 1.
22. J. Wyman, *J. Mol. Biol.*, 1965, **11**, 631.
23. M. N. Jones and P. Manley, *J. Chem. Soc., Faraday Trans. 1*, 1979, **75**, 1736.
24. J. Cordoba, M. D. Reboiras, and M. N. Jones, *Int. J. Biol. Macromol.*, 1988, **10**, 270.
25. M. N. Jones and P. Manley, in 'Surfactants in Solution', ed. K. L. Mittal and B. Lindman, Plenum Press, New York, 1984, Vol. 2, p. 1403.
26. W. Pfeil and P. L. Privalov, *Biophys. Chem.*, 1976, **4**, 41.
27. J. A. McCammon and S. C. Harvey, 'Dynamics of Proteins and Nucleic Acids', Cambridge University Press, Cambridge, 1987.
28. R. Diamond, D. C. Phillips, C. C. F. Blake, and A. C. T. North, *J. Mol. Biol.*, 1974, **82**, 371.
29. B. R. Brooks, R. E. Brucceroli, B. D. Olafson, D. J. States, S. Swaminathan, and M. Karplus, *J. Comp. Chem.*, 1985, **4**, 187.
30. J. A. McCammon, B. R. Gelin, and M. Karplus, *Nature (London)*, 1977, **267**, 585.
31. A. Yonath, A. Podjarny, B. Honig, A. Sielecki, and W. Traub, *Biochemistry*, 1977, **16**, 1418.